Newsjournal of the Society for Industrial and Applied Mathematics
sinews.siam.org

siam news

Volume 53/ Issue 2
March 2020

# Dandelion Seeds as Brilliant Parachutes

*By Jenny Morber*

People have long looked to nature to understand the secrets of flight. Leonardo da Vinci and the Wright brothers filled pages with observations on birds, Airbus now fits some jetliners with patches that mimic shark skin, and research groups are studying arrays of mini drones inspired by flies and bees. Yet only recently have we turned our attention to the lowly dandelion.

In 2018, researchers from the University of Edinburgh reported an interesting experimental finding on dandelion seeds [1]. They discovered that the soft filaments that radiate out from the dandelion seed stalk create a ring-shaped wake, which helps keep seeds aloft. Pier Giuseppe Ledda, Lorenzo Siconolfi, Francesco Viola, Simone Camarri, and François Gallaire extended that work by modeling the airflow around this structure, called the pappus [2]. Their study revealed the ideal number of filaments for maximum flight distance — the same number found in real seeds. It thus appears that the dandelion seed is optimized for steady cruising. This work represents a fascinating peek at an often-overlooked phenomenon and suggests the application of biologically-inspired designs for lightweight parachutes and aircraft instability challenges.

The team became interested in this mechanism when they observed an unusual separation between the top of the pappus and its air recirculation region (the area of circular flow behind impenetrable objects as they move through a fluid). Usually this vortex trails immediately behind. Blunt objects like trucks and barges have large recirculation regions, though designers strive for efficient aerodynamics to reduce the effect of the area of circular flow.

"When looking at the pictures of the dandelion seed that were produced by the group at Edinburgh, we were very surprised because while the seeds have a recirculation region, it is detached from the body," Camarri said. "If you look just past the body, the flow is not yet reversed. It reverses at the given distance, which is very peculiar." Camarri and his colleagues were able to attribute this anomaly to the porosity of the pappus. Like a parachute, the pappus must create enough drag to counterbalance the seed's weight, but it gains stability by letting some air through. Exactly how this worked in a dandelion seed was anybody's guess.

To tackle the problem, Ledda et al. combined linear stability analysis with an averaging technique for nonhomogeneous porous materials. They began by simplifying the pappus geometry. One can visualize the pappus as a wagon wheel and its filaments as thin cylindrical spokes. The area in the wheel's center where the spokes meet

*See* **Dandelion Seeds** *on page 4*

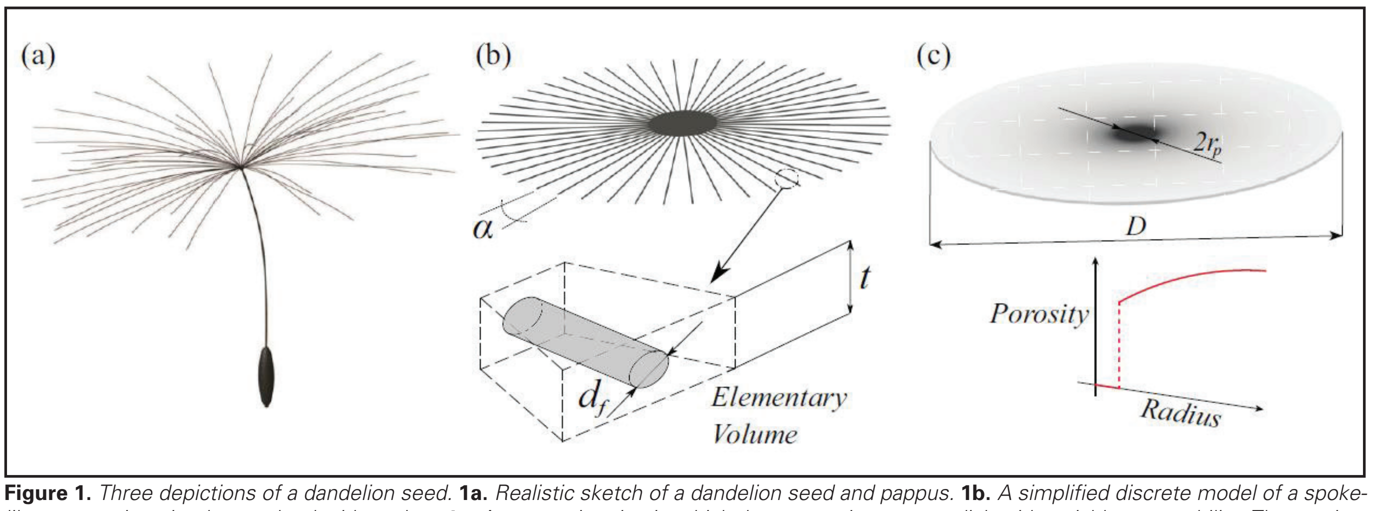


**Figure 1.** *Three depictions of a dandelion seed.* **1a.** *Realistic sketch of a dandelion seed and pappus.* **1b.** *A simplified discrete model of a spoke-like pappus, imagined as a wheel with spokes.* **1c.** *An approximation in which the pappus is a porous disk with variable permeability. The continuous porous disk models flow, where porosity and permeability are functions of the disk radius. Figure courtesy of [2].*

# How Zebrafish Get Their Stripes... or Spots

*By Alexandria Volkening and Björn Sandstede*

When we think of self-organization, flocking birds, swarming locusts, schooling fish, or traffic flow might come to mind. It is remarkable that the interactions of individual agents can yield reliable and diverse group dynamics across these systems. This is particularly true for biological self-organization at smaller scales. For example, healthy organism development relies on the careful interactions of different types of cells, and tissue-level properties emerge robustly as organisms grow despite the inherently noisy environments in which cells operate. Our work focuses specifically on cellular self-organization in zebrafish skin patterns.

These small freshwater fish have light and dark stripes across their bodies and fins (see Figure 1b). Interacting pigment cells—which migrate, differentiate, change color or shape, and compete on the growing skin—create the characteristic stripes. Much is unknown about these interactions. For instance, what signals cause a cell to change shape? What genes control cell interactions? How do genetic mutations alter behavior — and consequently, larger organism-scale features? We use modeling to predict the unknown cues that underlie newly-observed cell behaviors in zebrafish.

From a mathematical perspective, zebrafish skin patterning is a rich problem because it involves cell interactions at short and long range [7], and self-organization occurs as the fish grows (see Figures 1a and 1e). Zebrafish mutants also display a large range of altered skin patterns, including spots, labyrinth curves, and broken stripes. To better understand these patterns, modelers have focused on the interactions of two cell types: black melanophores and gold xanthophores. Previous models have included agent-based [2, 12], cellular automaton [1], and continuum approaches [4, 7], and these various techniques work together to provide different perspectives on pattern formation.

### New Cellular Players in Pattern Formation

Since the development of the aforementioned models, the empirical view of zebrafish patterns has undergone a paradigm shift [6, 8]. Until about 2014, the biological community focused only on melanophores and xanthophores. Researchers acknowledged a third type of pigment cell, called the iridophore, but assumed that these cells were unrelated to pattern formation because they are spread across the fish's entire body. Experimentalists have since observed that iridophores take on two different forms in light and dark stripes, and—strikingly—if iridophores fail to appear, zebrafish develop

*See* **Zebrafish** *on page 3*

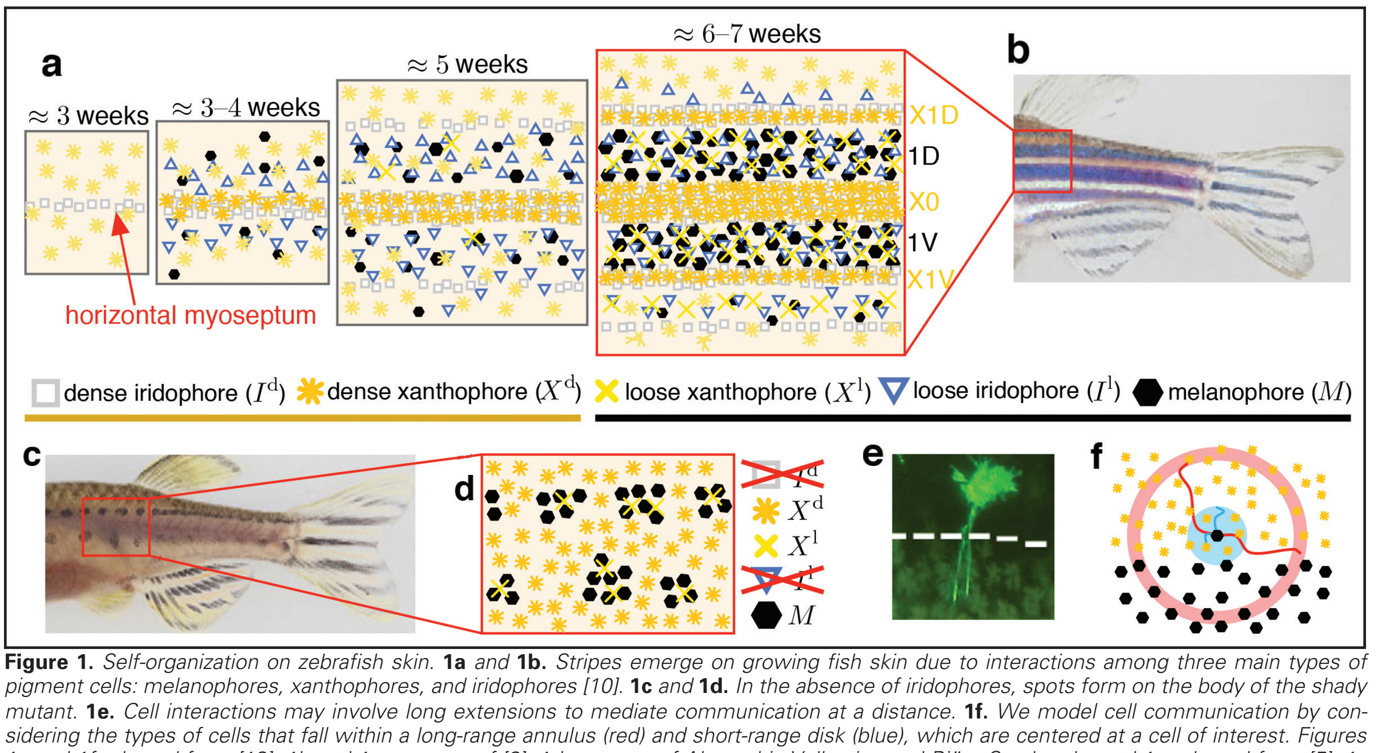


**Figure 1.** *Self-organization on zebrafish skin.* **1a** *and* **1b.** *Stripes emerge on growing fish skin due to interactions among three main types of pigment cells: melanophores, xanthophores, and iridophores [10].* **1c** *and* **1d.** *In the absence of iridophores, spots form on the body of the shady mutant.* **1e.** *Cell interactions may involve long extensions to mediate communication at a distance.* **1f.** *We model cell communication by considering the types of cells that fall within a long-range annulus (red) and short-range disk (blue), which are centered at a cell of interest. Figures 1a and 1f adapted from [13], 1b and 1c courtesy of [3], 1d courtesy of Alexandria Volkening and Björn Sandstede, and 1e adapted from [5]. 1a and 1f are licensed under CC-BY 4.0 (https://creativecommons.org/licenses/by/4.0/); and 1b, 1c, and 1e are licensed under CC-BY 3.0 (http://creativecommons.org/licenses/by/3.0) and published by the Company of Biologists Ltd.*

Nonprofit Org
U.S. Postage
PAID
Permit No 360
Bellmawr, NJ

siam
SOCIETY for INDUSTRIAL and APPLIED MATHEMATICS
3600 Market Street, 6th Floor
Philadelphia, PA 19104-2688 USA

siam news
Volume 53/ Issue 2/ March 2020



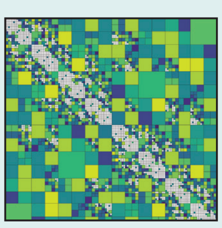



# *In Silico* Medicine Advances the Development of Sickle Cell Disease Therapies

*By He Li, Lu Lu, Peter Vekilov, and George Em Karniadakis*

Human red blood cells (RBCs) carry oxygen from the lungs to peripheral tissues and in turn transport carbon dioxide from tissues to the lungs for exhalation. RBCs, which are approximately 8 μm wide, undergo drastic deformations during their circulation in the human vasculature as they repeatedly pass through arterioles and capillaries as small as 2-3 μm.

Individuals with sickle cell disease (SCD) carry a genetic mutation in the gene for hemoglobin, a group of oxygen-binding proteins residing inside RBCs [9]. Under hypoxia, the mutated hemoglobin (HbS) can polymerize into stiff HbS fibers that distort the RBCs into various pathological shapes, ranging from elongated, granular, oval, and holly-leaf to crescent — the classic sickle shape [2]. In addition to the heterogeneous morphological changes, sickle RBCs also exhibit increased stiffness and adhesion; these features potentially contribute to the initiation and propagation of vaso-occlusion crises (VOCs), a hallmark of SCD. Recurrent and unpredictable episodes of VOC lead to stroke, frequent painful crises, and other serious complications like acute chest syndrome, splenic sequestration crisis, and acute liver crisis [10].

SCD affects roughly 100,000 people in the U.S. and millions worldwide. The disease is most prevalent among African Americans, afflicting one out of every 365 babies. Drug therapy is still the most affordable way to treat the majority of SCD patients. For 60 years, the cancer drug *Hydroxyurea* was the only available medication for SCD. The U.S. Food and Drug Administration (FDA) recently approved two new drugs: *Endari*, which is thought to reduce oxidative stress in RBCs, and *Adakveo*, which seems to prevent VOCs by reducing blood cell adhesion (a downstream target in SCD). However, no molecular-level mechanisms of these two drugs have been documented in the biomedical literature.

There is a pressing need to develop new drug therapies that target the sickling of RBCs — the root cause of SCD. Discovery and development of a novel drug is a long process that normally requires four to six years of laboratory experiments on human cells and animal models before it can enter clinical trials. Given recent advances in quantitative multiscale modeling for biological systems,[1] it is now possible to integrate traditional drug development approaches with *in silico* methods to accelerate laboratory studies and expeditiously explore new SCD drug targets.

## Mathematical Models

Our group has generated particle-based microscopic and mesoscopic models to simulate biological problems in SCD and improve our understanding of the disease's pathogenesis and pathophysiology. *At the microscopic level*, we created coarse-grained molecular dynamics (CGMD) HbS fiber models [6, 7] to simulate HbS molecules' self-assembly into fibers and the consequent fiber-fiber interaction. In parallel work, we developed OpenRBC [13], a CGMD code that uses a single shared memory commodity workstation to simulate an entire RBC at the molecular level. The simulation includes multiple millions of particles that explicitly represent the lipid bilayer and cytoskeleton. *At the mesoscopic level*, we produced dissipative particle dynamics (DPD) models of RBCs based on the rigorous theory of the Mori-Zwanzig formalism from statistical physics [5]. DPD-based RBC models enable us to simulate biological processes beyond the cellular level, such as the initiation of VOC by sickle RBCs in capillaries and venules [3].

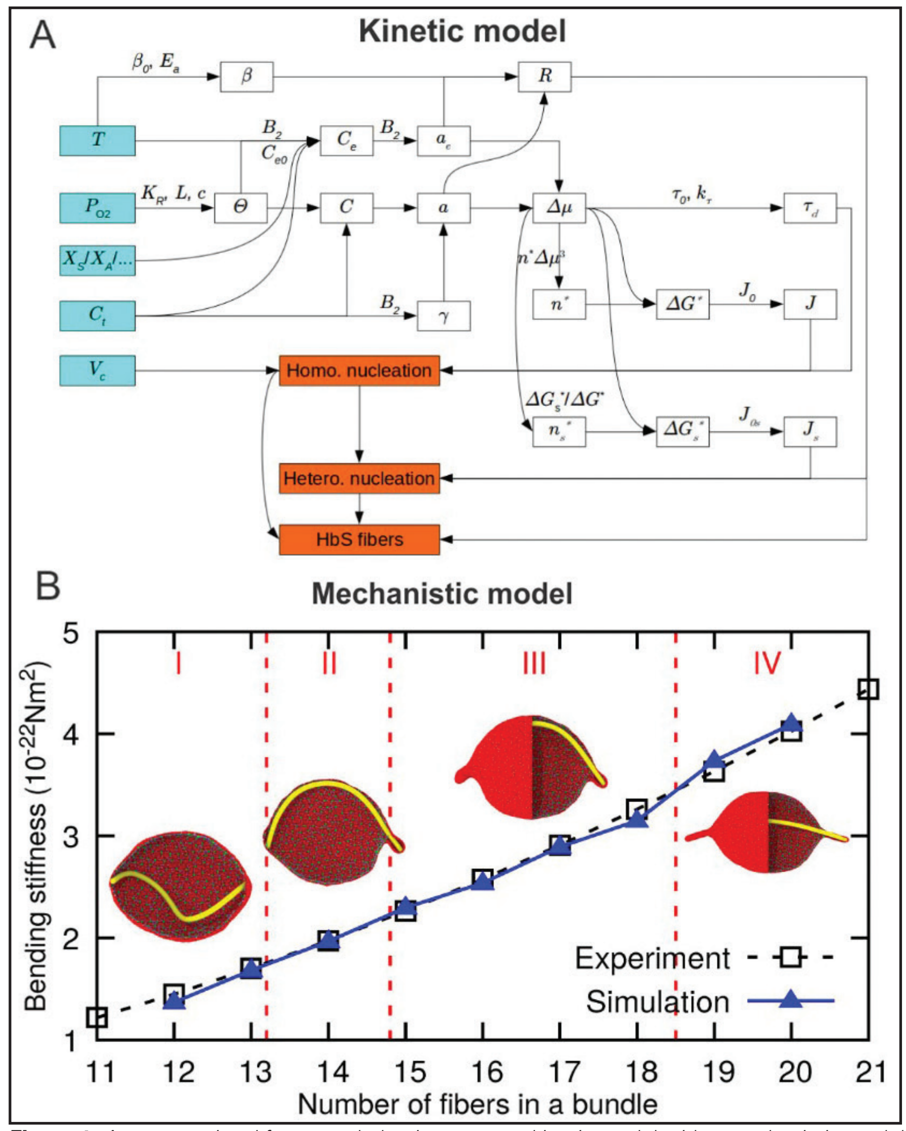


**Figure 1.** *A computational framework that integrates a kinetic model with a mechanistic model can predict the efficacy of anti-sickling drugs and discover new drug targets.* **1a.** *The kinetic model predicts the number of fibers inside red blood cells (RBCs) and the rate at which they grow under patient-specific and organ-specific conditions.* **1b.** *The mechanistic model determines the sickling of RBCs based on the kinetic model's outputs. Figure adapted from [8]. Refer to [8] for definitions of kinetic quantities in 1a.*

We recently put forth a kinetic model [8] based on classical nucleation theory to explicitly describe the kinetics of HbS molecules' homogeneous and heterogeneous nucleation, as well as the growth dynamics of HbS fibers. Our team built a computational framework by integrating this kinetic model with our mechanistic model to assess potential SCD drugs and individualized pathology (see Figure 1).

### *In Silico* Analysis for Enhanced Drug Development

We validated this new framework by demonstrating that our model predictions are consistent with prior *in vivo* [11] and *in vitro* studies [1, 4]. In particular, our model can predict the SCD drug efficacy in agreement with the drug screening assay in Figures 2a and 2b (on page 5), where each point of the experimental data (black symbols) represents 12 measurements with durations of either four or 24 hours [4] — not including experimental setup time. On the other hand, it only takes about one minute to obtain the corresponding simulation results (blue symbols) by running the computational model on a laptop computer. Given this high efficiency, researchers can use computational modeling as an extra drug pre-screening modality to reduce the number of experimental tests without compromising measurement reliability. This accelerates laboratory studies before new drugs enter expensive clinical trials.

We performed a *global* sensitivity analysis of sickled fractions of RBCs to the model's kinetic quantities to identify key quantities for consideration as potential druggable targets. We employed variance functional decomposition [12]—in which we simultaneously varied 13 quantities—to conduct this analysis. As shown in Figures 2c and 2d (on page 5), our global sensitivity analysis indicates that RBC sickling is sensitive to hemoglobin solubility $(C_{e0})$, nucleation rate pre-factor $(J_0)$, oxygen-binding affinity $(K_R)$, and hemoglobin activity $(B_2)$. These findings provide therapeutic rationales for anti-sickling targets, which are consistent with previous findings but also identify new druggable targets. For example, a new anti-sickling drug called *Voxelotor*—recently approved by the FDA

*See* **Sickle Cell Disease** *on page 5*

[1] https://www.imagwiki.nibib.nih.gov/

siam news

ISSN 1557–9573. 

# Third Biennial SIAM Conference on Applied Mathematics Education to Coincide with MAA MathFest in July 2020

*By Ron Buckmire and Karen Bliss*

For the first time, the SIAM Conference on Applied Mathematics Education[1] (ED20) will be co-located with the Mathematical Association of America's (MAA) MathFest.[2] MathFest will begin on July 29 and ED20 will commence on July 30, with both events concluding on August 1 in Philadelphia, Penn. ED20 marks the third iteration of the biennial conference. The meeting was paired with the SIAM Conference on Mathematics of Planet Earth in Philadelphia in 2016, and with the SIAM Annual Meeting in Portland, Ore., in 2018.

This year's conference is a unique collaboration between SIAM and another national mathematics association. MathFest is the MAA's summer meeting — a venue for presentations on research in mathematics and mathematics education that is also particularly welcoming to both undergraduate and graduate students. As indicated on the meeting's website, ED20 is "intended for mathematics teacher educators, especially for in-service professional development; faculty members in colleges and universities who are interested in applied and computational mathematics and have a strong interest in educational innovation, practice, improvement, and faculty development; and graduate students in applied mathematical areas with ambitions for careers in academia with a strong education component." The conference is sponsored by the SIAM Activity Group on Applied Mathematics Education, and the organizing committee consists of a dozen applied mathematics professors and professionals from a diverse set of institutions, led by Karen Bliss (Virginia Military Institute) and Ron Buckmire (Occidental College).

With the MAA exiting its agreement with the American Mathematical Society for shared stewardship of the Joint Mathematics Meetings after 2021, MathFest's importance in the annual calendar of national mathematics meetings is increasing. Other events will likely co-locate with MathFest—beginning with ED20 this year—in future years.

The themes of ED20 are as follows: Educating Students in Applied Mathematics; Issues of Equity, Diversity, and Inclusion in Applied Mathematics; Mathematical Modeling Inside and Outside the Classroom; Engaging the Public in Applied Mathematics; and Scholarship and Research in Applied Mathematics Education.

Invited speakers for the conference include Chad Topaz (Williams College), who will present the SIAM-MAA Joint Invited Presentation, as well as Brynja Kohler (Utah State University), Chris Rasmussen (San Diego State University), Cristina Villalobos (University of Texas Rio Grande Valley), and Darryl Yong (Harvey Mudd College).

ED20 attendees have until March 6 to submit minisymposia abstracts and until April 30 to submit contributed papers. They must register for the conference by June 30.

*Ron Buckmire is a professor of mathematics and Associate Dean for Curricular Affairs at Occidental College. Karen Bliss is an associate professor in the Department of Applied Mathematics at Virginia Military Institute.*

[1] https://www.siam.org/conferences/cm/conference/ed20

[2] https://www.maa.org/meetings/mathfest

## Zebrafish

*Continued from page 1*

spots instead of stripes (see Figures 1c and 1d, on page 1) [3, 9, 11].

To form stripes, iridophores diffuse outward from a central horizontal marker on the body [3, 11]. As they spread, they transform in color and shape between dense (silver) and loose (blue) (see Figure 1a, on page 1). These transitions are critical: when dense iridophores become loose, they signal the formation of a new dark stripe; black melanophores then emerge in this area. On the other hand, gold xanthophores react and new light stripes emerge in places where spreading loose iridophores become dense.

It is now clear that iridophores help direct black and gold cells by changing their shape and color. But what signals instruct them to do so? To help answer this question, we developed an agent-based model [13] that accounts for all three main types of pigment cells. We included two subtypes of xanthophores and iridophores, allowing these cells to adopt dense or loose forms (see Figure 1a, on page 1). Broadly, we model cells as point masses and couple deterministic migration with stochastic, discrete-time rules for cell birth, death, and shape/color changes. Our model simulates the timeline of pattern development on growing domains (see Figure 1a, on page 1).

We describe cell migration with ordinary differential equations using a kinematic approximation; for example, the movement of the $i$th black cell with position $\mathbf{M}_i(t)$ is given by

$$\frac{d\mathbf{M}_i}{dt} = \underbrace{\sum_{\text{other } M \text{ cells}} F^{MM}(\|\mathbf{M}_j - \mathbf{M}_i\|)\frac{\mathbf{M}_j - \mathbf{M}_i}{\|\mathbf{M}_j - \mathbf{M}_i\|}}_{\text{repulsion from melanophores } (M)} + \underbrace{\sum_{X^{\mathrm{d}} \text{ cells}} F^{X^{\mathrm{d}}M}(\|\mathbf{X}_j^{\mathrm{d}} - \mathbf{M}_i\|)\frac{\mathbf{X}_j^{\mathrm{d}} - \mathbf{M}_i}{\|\mathbf{X}_j^{\mathrm{d}} - \mathbf{M}_i\|}}_{\text{repulsion from dense xanthophores } (X^{\mathrm{d}})} + \underbrace{\sum_{I^{\mathrm{d}} \text{ cells}} F^{I^{\mathrm{d}}M}(\|\mathbf{I}_j^{\mathrm{d}} - \mathbf{M}_i\|)\frac{\mathbf{I}_j^{\mathrm{d}} - \mathbf{M}_i}{\|\mathbf{I}_j^{\mathrm{d}} - \mathbf{M}_i\|}}_{\text{weak repulsion from dense iridophores } (I^{\mathrm{d}})}.$$

Here, $\mathbf{X}_j^{\mathrm{d}}(t)$ and $\mathbf{I}_j^{\mathrm{d}}(t)$ are the positions of the $j$th dense xanthophore and iridophore respectively, and

$$F^{\mu\nu}(d) = -R^{\mu\nu}\left(\frac{1}{2} + \frac{1}{2}\tanh\left(\frac{r_{\mu\nu} - d}{\delta}\right)\right)$$

is a repulsive or attractive force. Our rules for cell birth, death, and form changes are in turn given by inequalities that must be satisfied for specific behaviors to occur. These inequalities depend on the types of cells in different interaction neighborhoods. For example, we specify that the $i$th silver iridophore at position $\mathbf{I}_i^{\mathrm{d}}$ becomes loose when there are sufficient black cells in a ball ($B^{\mathbf{I}_i^{\mathrm{d}}}$) centered around it:

$$\sum_{M \text{ cells}} \mathbb{1}_{B^{\mathbf{I}_i^{\mathrm{d}}}}(\mathbf{M}_j) > 3 \text{ cells} \Rightarrow \text{dense iridophore at position } \mathbf{I}_i^{\mathrm{d}} \text{ transforms to loose.} \tag{1}$$

Our full model [13] combines rules with this general flavor, and in some cases involves nonlinear combinations of conditions that must be met simultaneously for given cell behaviors to occur.

Specifying parameters and rules in agent-based models is often tricky. To address this challenge, we first utilized the wealth of literature on melanophores and xanthophores, the two original cell types. We based our parameters for migration, birth, and death on empirical measurements and past experiments; for these interactions, one can view our model as descriptive rather than predictive. This left us to specify the rules for iridophore-form transitions, which are poorly understood but critical for the formation of new stripes.

### Puzzling out Signals that Cells Receive to Change Their Clothes

To address the paucity of information on iridophores, we split the biological data into distinct sets for model derivation and evaluation. Zebrafish display a few major types of mutant patterns, which provided a natural means of dividing the data. Studying the development of wild-type fish and mutants lacking cell types (our *derivation set*) allowed us to identify possible mechanisms that might be governing iridophore-form transitions. The first class of mutants features altered patterns simply because a cell type fails to appear. Only one of our proposed mechanisms was capable of reproducing our full derivation set. We checked our model by testing its performance on our *evaluation set*: a series of well-understood mutants and experiments. We found good agreement across the last 15 years of biological data.

We concluded that iridophores depend on a complex, nonlinear combination of redundant cues from black melanophores and gold xanthophores (at short and long range) to change their shape. From a mathematical viewpoint we were hoping for more elegant rules, so we tried breaking down our iridophore mechanisms into their simpler components, as in (1). This led to an unfamiliar pattern: light spots on a dark background (see Figure 2a). Many zebrafish mutants have black spots, but none display light spots. Instead, the pattern we found resembles *Danio margaritatus*, a relative of zebrafish. We therefore suggest that the complex, redundant nature of iridophore interactions might provide a source of pattern variability in closely-related fish.

### Striped *and* Spotted Fish?

Although mutant zebrafish that lack iridophores feature spots on their bodies, this does not occur on the fins: light and dark stripes form just fine on fins based on interactions between the original two cell types (see Figures 1c and 1d, on page 1). We are currently exploring how different environments on the fish body and fins may lead to spots in one region but stripes in another. How do the pigment cells in spots and stripes interact across pattern interfaces? Many questions remain, and we expect that biological and mathematical perspectives on zebrafish patterning will continue to evolve together.

### References

[1] Bullara, D., & De Decker, Y. (2015). Pigment cell movement is not required for generation of Turing patterns in zebrafish skin. *Nat. Commun., 6*, 6971.

[2] Caicedo-Carvajal, C.E., & Shinbrot, T. (2008). *In silico* zebrafish pattern formation. *Dev. Biol., 315*, 397-403.

[3] Frohnhöfer, H.G., Krauss, J., Maischein, H.-M., & Nüsslein-Volhard, C. (2013). Iridophores and their interactions with other chromatophores are required for stripe formation in zebrafish. *Develop., 140*(14), 2997-3007.

[4] Gaffney, E., & Lee, S.S. (2013). The sensitivity of Turing self-organization to biological feedback delays: 2D models of fish pigmentation. *Math. Med. Biol., 32*(1), 56-78.

[5] Hamada, H., Watanabe, M., Lau, H.E., Nishida, T., Hasegawa, T., Parichy, D.M., & Kondo, S. (2014). Involvement of delta/notch signaling in zebrafish adult pigment stripe patterning. *Develop., 141*(2), 318-324.

[6] Kondo, S., & Watanabe, M. (2015). Black, yellow, or silver: Which one leads skin pattern formation? *Pigment Cell Melanoma Res., 28*, 2-4.

[7] Nakamasu, A., Takahashi, G., Kanbe, A., & Kondo, S. (2009). Interactions between zebrafish pigment cells responsible for the generation of Turing patterns. *Proc. Natl. Acad. Sci. U.S.A., 106*, 8429-8434.

[8] Nüsslein-Volhard, C., & Singh, A.P. (2017). How fish color their skin: A paradigm for development and evolution of adult patterns. *BioEssays, 39*(3).

[9] Patterson, L.B., & Parichy, D.M. (2013). Interactions with iridophores and the tissue environment required for patterning melanophores and xanthophores during zebrafish adult pigment stripe formation. *PLoS Genet., 9*, e1003561.

[10] Singh, A.P., & Nüsslein-Volhard, C. (2015). Zebrafish stripes as a model for vertebrate colour pattern formation. *Curr. Biol., 25*, R81-R92.

[11] Singh, A.P., Schach, U., & Nüsslein-Volhard, C. (2014). Proliferation, dispersal and patterned aggregation of iridophores in the skin prefigure striped colouration of zebrafish. *Nat. Cell Biol., 16*, 604-611.

[12] Volkening, A., & Sandstede, B. (2015). Modelling stripe formation in zebrafish: an agent-based approach. *J. Roy. Soc. Interface, 12*, 20150812.

[13] Volkening, A., & Sandstede, B. (2018). Iridophores as a source of robustness in zebrafish stripes and variability in *Danio* patterns. *Nat. Commun., 9*, 3231.

*Alexandria Volkening is an NSF-Simons Fellow in the NSF-Simons Center for Quantitative Biology and the Department of Engineering Sciences and Applied Mathematics at Northwestern University. Björn Sandstede is a professor of applied mathematics, a Royce Family Professor of Teaching Excellence, and director of the Data Science Initiative at Brown University.*

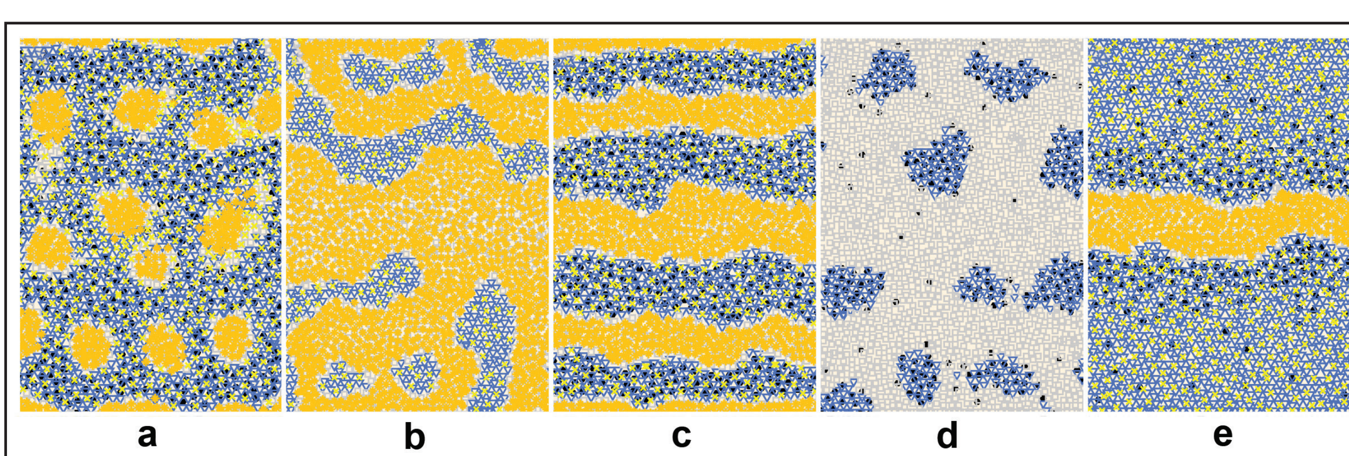


**Figure 2.** *Example of pattern diversity. Model simulations of the following:* **2a.** *Danio margaritatus.* **2b.** *Mutant nacre zebrafish.* **2c.** *Wild-type zebrafish (Danio rerio).* **2d.** *Mutant pfeffer zebrafish.* **2e.** *Danio albolineatus. Figure adapted from [13]; individual images licensed under CC-BY 4.0 (https://creativecommons.org/licenses/by/4.0/).*

## Dandelion Seeds

*Continued from page 1*

is impermeable, but air can pass through the spokes in the outer region (see Figure 1, on page 1). Varying the number of spokes or filaments ($n_f$) and their diameter ($d_f$) changes the porosity of the pappus.

The researchers defined a cylindrical coordinate system $(x, r, \theta)$ with its origin at the disk center and $r$ as the radial direction. The $x$-direction is parallel to the inflowing air velocity. The porosity of the pappus is then

$$\phi(r) = 1 - \frac{n_f d_f^2}{8tr},$$

where $t$ is the disk thickness and $r$ is the disk radius. The mean porosity is the ratio between the area of the disk's spokes and the disk's total area, written as

$$\Phi = 1 - \frac{n_f d_f (D/2 - r_p) + \pi r_p^2}{\pi (D/2)^2}.$$

Here, $r_p$ is the radius of the inner, impermeable region (the pulvinus) and $D$ is the diameter of the entire disk. The researchers explored a wide range of mean porosities, keeping $d_f$ constant while varying $n_f$ (see Figure 2).

One can therefore treat the pappus as a nonhomogeneous rigid porous disk with an impermeable center. Ledda et al. performed a global stability analysis of the pappus using the unsteady incompressible Navier-Stokes equations:

$$\partial tu + u \cdot \nabla u + \nabla p - \frac{1}{Re}\nabla^2 u = 0$$

$$\nabla \cdot u = 0,$$

where $u$ is the velocity vector, $p$ is the pressure field, and $Re$ is the Reynolds number for fluid viscosity. The latter is defined as $Re = U\infty D/v$, where $v$ is the fluid's kinematic viscosity. In the porous region, average quantities describe the fluid's motion according to a model based on a Brinkman formulation:

$$\frac{1}{\phi}\partial_t \boldsymbol{u} + \frac{1}{\phi^2}\boldsymbol{u} \cdot \nabla \boldsymbol{u} + \nabla p - \frac{1}{\phi Re}\nabla^2 \boldsymbol{u} +$$

$$\frac{1}{Re}\boldsymbol{Da}^{-1}\boldsymbol{u} = \boldsymbol{0}, \qquad \nabla \cdot \boldsymbol{u} = \boldsymbol{0}.$$

Here, $\boldsymbol{Da}$ is a nondimensional permeability tensor. These equations are completed by imposing Dirichlet boundary conditions on the air inlet and lateral boundaries, stress-free requirements on the outflow boundary, and velocity and pressure continuity at fluid-solid interface boundaries.

Using a linear stability approach, the flow can be decomposed as $q = Q_b(x,r) + \varepsilon q'(x,r,\theta,t)$, where $Q_b = (U_b, p_b)$ is the "base flow" and $q' = (u', p')$ is the unsteady perturbation with amplitude $\varepsilon \ll 1$. This flow decomposition yields at zero order the base flow steady governing equations and $U_{br} = \partial U_{bx}/\partial r = 0$ for axisymmetric solutions.

At order $\varepsilon^1$ an unstable perturbation evolves, which expands in Fourier modes in the azimuthal direction $\boldsymbol{q}'(x,r,\theta,t) = q\hat{}(x,r)\exp(im\theta + \sigma t)$, where $m$ is the azimuthal wave number and $\sigma$ is a complex number with the perturbation growth rate as its real part and the frequency as its imaginary part. The resulting eigenvalue in the fluid region then becomes

$$\sigma\hat{\boldsymbol{u}} + \boldsymbol{U}_b \cdot \nabla_m \hat{\boldsymbol{u}} + \hat{\boldsymbol{u}} \cdot \nabla_0 \boldsymbol{U}_b + \nabla_m \hat{\boldsymbol{p}} -$$

$$\frac{1}{Re}\nabla_m^2 \hat{\boldsymbol{u}} = \boldsymbol{0}, \qquad \nabla_m \cdot \hat{\boldsymbol{u}} = \boldsymbol{0},$$

and can be written as

$$\frac{1}{\phi}\sigma\hat{\boldsymbol{u}} + \frac{1}{\phi^2}(\boldsymbol{U}_b \cdot \nabla_m \hat{\boldsymbol{u}} + \hat{\boldsymbol{u}} \cdot \nabla_0 \boldsymbol{U}_b) +$$

$$\nabla_m \hat{p} - \frac{1}{\phi Re}\nabla_m^2 \hat{\boldsymbol{u}} + \frac{1}{Re}\boldsymbol{Da}^{-1}\hat{\boldsymbol{u}} = \boldsymbol{0},$$

$$\nabla_m \cdot \hat{\boldsymbol{u}} = \boldsymbol{0}$$

in the porous region. The operators are defined as

$$\nabla_m p = \begin{bmatrix} \frac{\partial p}{\partial x} \\ \frac{\partial p}{\partial r} \\ \frac{imp}{r} \end{bmatrix},$$

$$\nabla_m \boldsymbol{u} = \begin{bmatrix} \frac{\partial u_x}{\partial x} & \frac{\partial u_x}{\partial r} & \frac{im}{r}u_x \\ \frac{\partial u_r}{\partial x} & \frac{\partial u_r}{\partial r} & \frac{im}{r}u_r - \frac{u_\theta}{r} \\ \frac{\partial u_\theta}{\partial x} & \frac{\partial u_\theta}{\partial r} & \frac{im}{r}u_\theta + \frac{u_r}{r} \end{bmatrix},$$

$$\nabla_m \cdot \boldsymbol{u} = \frac{\partial u_x}{\partial x} + \frac{1}{r}\frac{\partial (ru_r)}{\partial r} + \frac{im}{r}u_\theta,$$

and

$$\nabla_m^2 \boldsymbol{u} = \nabla_m \cdot (\nabla_m \boldsymbol{u}).$$

The researchers set the displacement mode to $m = 1$, which corresponds to the first instability in an axisymmetric wake past a circular flat disk set normal to the fluid flow [3]. This displacement mode requires axis regularity conditions

$$\frac{\partial \hat{u}_r}{\partial r} = \hat{u}_x = \frac{\partial \hat{u}_\theta}{\partial r} = 0.$$

The open-source software `FreeFem++`—with 200,000 degrees of freedom and boundaries at $r\infty = 20$, $x - \infty = -25$, and $x + \infty = 50$—yielded numerical solutions. The pulvinus is treated as a solid boundary with $u = 0$ on its border.

The team determined steady flow solutions $Q_b$ for dandelion seeds with different numbers of filaments: $n_f = 130$, 100, and 50, with $Re$ fixed at 400. Given this analysis, solutions to the flow equations indicate vortex rings that are partially detached from the disk base. The recirculation region remains partially attached in the impermeable pulvinus region (see Figure 3).

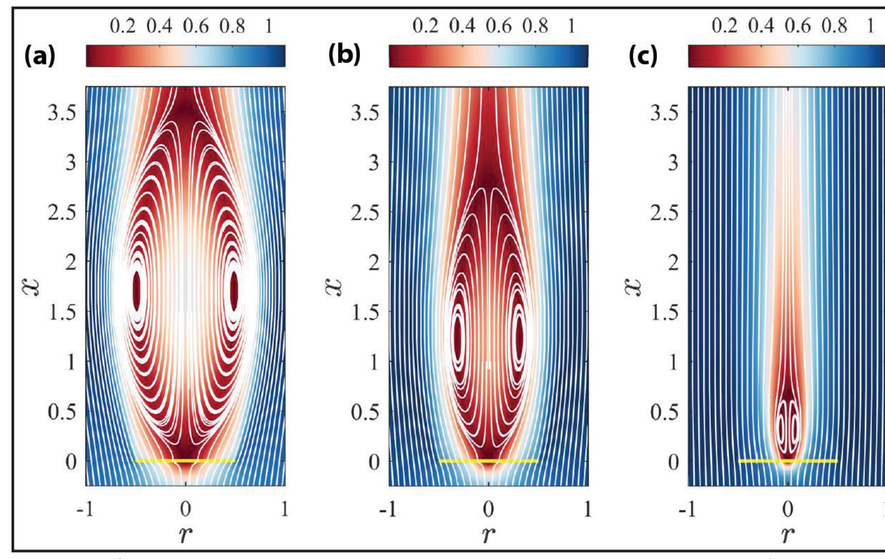


**Figure 3.** *Contour images showing steady and axisymmetric solutions to the flow equations for the following:* **3a.** $n_f = 130$ ($\phi = 0.911$). **3b.** $n_f = 100$ ($\phi = 0.931$). **3c.** $n_f = 50$ ($\phi = 0.964$). *The isocontours represent the velocity magnitude. Figure courtesy of [2].*

$Re$ is varied in the stability analysis. In the area of the disk, permeability increases as the number of filaments decreases, which affects the apparent fluid viscosity. Hence the local $Re$ strongly depends on disk permeability. As $Re$ increases, the wake shows two successive helical bifurcations: a steady initial bifurcation and a second one that is periodic in time.

Ledda et al. find a critical $Re$, past which instability is constant and equal to an impermeable disk. This critical value increases to an average permeability $\phi$ of approximately 0.93, at which the neutral stability curves diverge. Flow is thus even and linearly stable for porosity greater than 0.93, which occurs when the number of filaments equals 100. Interestingly, real dandelions typically carry 100 filaments; this suggests that a dandelion seed is optimized for steady and stable flight. Its filaments maximize drag until they begin to affect stability. "It's very exciting to find in nature something that resembles an optimal principle," Camarri said.

The researchers consider the pappus filaments to be rigid, but as anyone who has nuzzled a dandelion seed can attest, they are actually soft and pliable. Future studies could add more realistic refinements, such as accounting for filament deformation or modeling the seed in free flight with greater perturbations and lateral motion.

Ultimately, this work can help scientists study the dispersal of seeds or other similarly-sized objects in the air. Viscosity and length scales are important for applications based on these findings because small objects like dandelion seeds interact differently in the air than larger objects. The interplay between air viscosity and seed size makes this solution work. "It's kind of magic," Camarri said. "If you look at the volume occupied by the filaments with respect to the disk, we could more or less call it empty. Its ability to fly is therefore amazing."

### References


[1] Cummins, C., Seale, M., Macente, A., Certini, D., Mastropaolo, E.,Viola, I.M., & Nakayama, N. (2018). A separated vortex ring underlies the flight of the dandelion. *Nature, 562*(7727).

[2] Ledda, P.G., Siconolfi, L., Viola, F., Camarri, S., & Gallaire, F. (2019). Flow dynamics of a dandelion pappus: A linear stability approach. *Phys. Rev. Fluids, 4*, 071901.

[3] Meliga, P., Chomaz, J.-M., & Sipp, D. (2009). Unsteadiness in the wake of disks and spheres: Instability, receptivity and control using direct and adjoint global stability analyses. *J. Fluids Struct., 25*, 601.


*Jenny Morber holds a B.S. and Ph.D. in materials science and engineering from the Georgia Institute of Technology. She is a professional freelance science writer and journalist based out of the Pacific Northwest.*

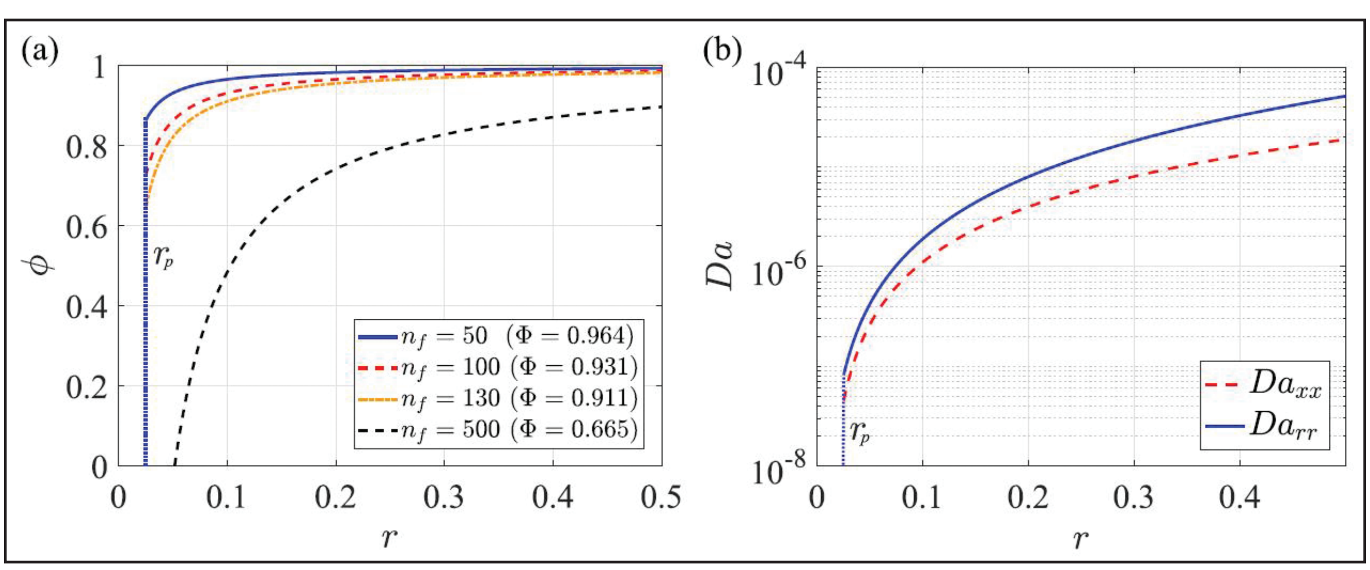


**Figure 2.** *Plots depicting porosity distribution for different numbers of pappus filaments* ($n_f$) (**2a**) *and permeability variation along the radius when* $n_f = 100$ (**2b**). *Da is a nondimensional permeability tensor. Figure courtesy of [2].*

# New SIAM Science Policy Fellowships Announced

SIAM's Science Policy Fellowship Program[1] engages early-career professionals in science policy and advocacy. Fellowship recipients learn about the workings of science policy as it pertains to our discipline by participating in SIAM's Committee on Science Policy[2] (CSP) meetings and conducting relevant activities to further SIAM's science policy efforts.

The 2020 Fellowship recipients are as follows:

- Samantha Erwin, *Oak Ridge National Laboratory*
- Michael Schneier, *University of Pittsburgh*
- Alyson Fox, *Lawrence Livermore National Laboratory*
- George Slota, *Rensselaer Polytechnic Institute*
- Luis Sordo Vieira, *The Jackson Laboratory**
- Andy Huang, *Sandia National Laboratories**
- Anthony Bonifonte, *Denison University**

Fellowships will pay for travel to the biannual SIAM CSP meetings. Each spring, the CSP meets with representatives of agencies (such as the National Science Foundation and the Department of Energy) that are relevant to our discipline and visits congressional offices to promote the importance of research funding, graduate training, and undergraduate education in applied mathematics and computational science.

*indicates Fellowship recipient who is completing the second year of his/her fellowship in 2020.

1 https://www.siam.org/students-education/programs-initiatives/siam-science-policy-fellowship-program
2 https://www.siam.org/about-siam/committees/committee-on-science-policy-csp

## Sickle Cell Disease

*Continued from page 2*

for an accelerated clinical trial—functions by increasing the oxygen-binding affinity, one of four targets identified by our model. Furthermore, our model can provide quantitative guidance on the required modification levels of these four kinetic quantities to achieve therapeutic efficacy.

The clinical outcomes of SCD drugs are heterogeneous [14]. This heterogeneity may be due to the variation in patient-specific RBC variables—like hemoglobin distribution and composition, and mean cell volume—as well as organ-specific environmental variables such as temperature, deoxygenation time, and initial and final oxygen pressure. Our computational framework enables predictions of RBC sickling using both patient- and organ-specific data, which opens the path to monitoring disease progression for individual SCD patients with various degrees of severity. Such model predictions can help clinicians make patient-specific prognoses and offer guidance on the optimal time for medical intervention. Our kinetic model can also provide direction for drug dosage based on patient-specific data, thus facilitating the development of precision medicine to eliminate the side effects of SCD drugs.

**Acknowledgments:** This work was supported by National Institutes of Health grant U01HL114476. The authors thank Ming Dao at the Massachusetts Institute of Technology; Pankaj Qasba at the National Heart, Lung, and Blood Institute; and Grace Peng at the National Institute of Biomedical Imaging and Bioengineering for helpful discussions.

### References

[1] Du, E., Diez-Silva, M., Kato, G.J., Dao, M., & Suresh, S. (2015). Kinetics of sickle cell biorheology and implications for painful vasoocclusive crisis. *Proc. Nat. Acad. Sci., 112*(5), 1422-1427.

[2] Ferrone, F.A. (2004). Polymerization and sickle cell disease: A molecular view. *Microcirc., 11*(2), 115-128.

[3] Lei, H., & Karniadakis, G.E. (2013). Probing vasoocclusion phenomena in sickle cell anemia via mesoscopic simulations. *Proc. Nat. Acad. Sci., 110*(28), 11326-11330.

[4] Li, Q., Henry, E.R., Hofrichter, J., Smith, J.F., Cellmer, T., Dunkelberger, E.B., …, Eaton, W.A. (2017). Kinetic assay shows that increasing red cell volume could be a treatment for sickle cell disease. *Proc. Nat. Acad. Sci., 114*(5), E689-E696.

[5] Li, Z., Bian, X., Caswell, B., & Karniadakis, G.E. (2014). Construction of dissipative particle dynamics models for complex fluids via the Mori-Zwanzig formulation. *Soft Matt., 10*(43), 8659-8672.

[6] Lu, L., Li, H., Bian, X., Li, X., & Karniadakis, G.E. (2017). Mesoscopic adaptive resolution scheme toward understanding of interactions between sickle cell fibers. *Biophys. J., 113*(1), 48-59.

[7] Lu, L., Li, X., Vekilov, P.G., & Karniadakis, G.E. (2016). Probing the twisted structure of sickle hemoglobin fibers via particle simulations. *Biophys. J., 110*(9), 2085-2093.

[8] Lu, L., Li, Z., Li, H., Li, X., Vekilov, P.G., & Karniadakis, G.E. (2019). Quantitative prediction of erythrocyte sickling for the development of advanced sickle cell therapies. *Sci. Advan., 5*(8), eaax3905.

[9] Pauling, L., Itano, H.A., Singer, S.J., & Wells, I.C. (1949). Sickle cell anemia, a molecular disease. *Science, 110*(2865), 543-548.

[10] Piel, F.B., Steinberg, M.H., & Rees, D.C. (2017). Sickle cell disease. *New Eng. J. Med., 376*(16), 1561-1573.

[11] Serjeant, G.R., Petch, M.C., & Serjeant, B.E. (1973). The *in vivo* sickle phenomenon: A reappraisal. *J. Lab. Clin. Med., 81*(6), 850-856.

[12] Sobol, I.M. (2001). Global sensitivity indices for nonlinear mathematical models and their Monte Carlo estimates. *Math. Comput. Sim., 55*(1-3), 271-280.

[13] Tang, Y.-H., Lu, L., Li, H., Evangelinos, C., Grinberg, L., Sachdeva, V., & Karniadakis, G.E. (2017). OpenRBC: A fast simulator of red blood cells at protein resolution. *Biophys. J., 112*(10), 2030-2037.

[14] Ware, R.E. (2015). Optimizing hydroxyurea therapy for sickle cell anemia. *ASH Edu. Prog. Book, 2015*(1), 436-443.

*He Li is a research assistant professor in the Division of Applied Mathematics at Brown University. Lu Lu is a senior Ph.D. and master's student in computer science in the Division of Applied Mathematics at Brown. Peter Vekilov is a John and Rebecca Moores Professor of Chemical and Biomolecular Engineering and of Chemistry at the University of Houston. He is a fellow of the American Physical Society. George Em Karniadakis is the Charles Pitts Robinson and John Palmer Barstow Professor of Applied Mathematics at Brown. He is a SIAM Fellow.*

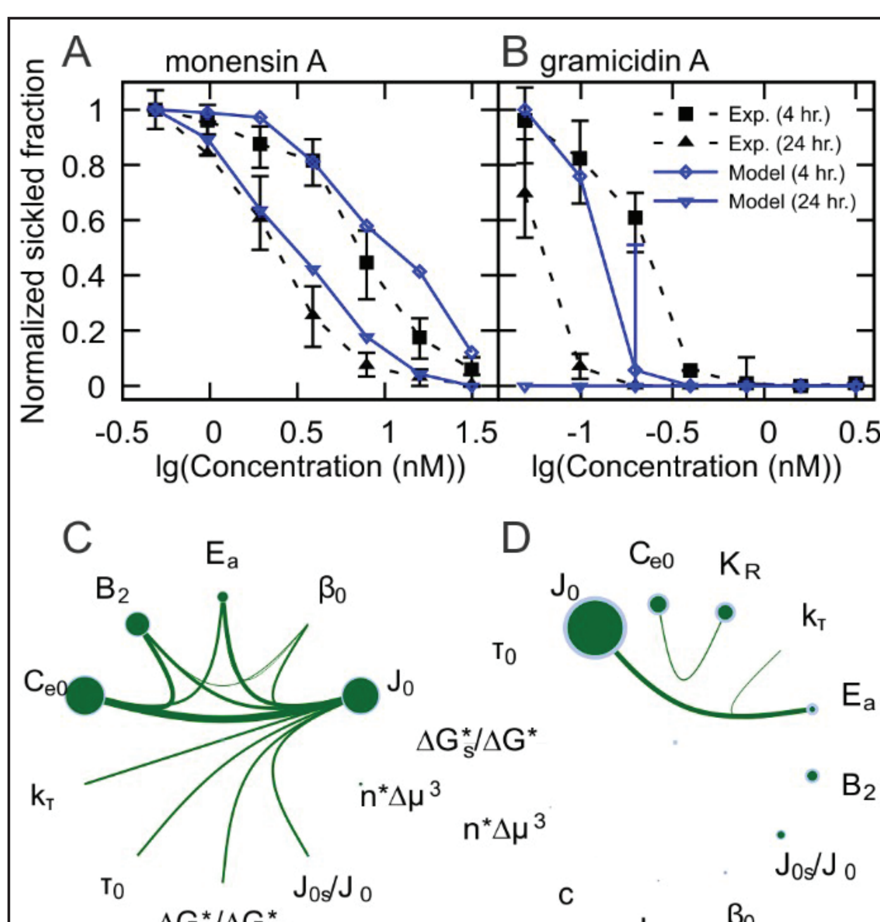


**Figure 2.** *Selection of critical parameters via global sensitivity analysis.* **2a** *and* **2b.** *The fraction of sickled red blood cells (RBCs) decreases with increased dosage of anti-sickling agents monensin A (2a) and gramicidin A (2b). Blue curves represent our simulation results and black curves denote the experimental results reported in [4]. Squares and diamonds correspond to four-hour incubations, and triangles correspond to 24-hour incubations.* **2c** *and* **2d.** *Global parametric sensitivity analysis on the kinetic quantities with model inputs following an in vitro study (2c) [4] and an in vivo study (2d) [11]. The diameter of the green circles is the first-order sensitivity index of each parameter. The blue ring surrounding the green circles represents the sensitivity index's 95 percent confidence interval. The line thickness between two parameters indicates the second-order sensitivity index of each two-parameter pair. Figure adapted from [8].*

# Wronskian = Angular Momentum; Abel's Formula = Newton's Second Law

Figure 1 depicts a point mass $m{=}1$ moving in a plane, pulled into the origin by a Hookean spring and subject to friction that is linear in velocity. Position $z\in\mathbb{R}^2$ obeys Newton's second law,

$$\ddot{z}=-qz-p\dot{z}. \qquad (1)$$

We allow $q$ and $p$ to depend on time (so that "Hooke's constant" $q=q(t)$ is constant only in $z$ but not necessarily in $t$).

On the one hand, taking the two-dimensional cross product with $z$ yields the evolution of the angular momentum $L=z\times\dot{z}$:

$$\frac{d}{dt}(z\times\dot{z})=-p\,(z\times\dot{z}). \qquad (2)$$

On the other hand, the coordinates of $z=(x,y)$ satisfy the same ordinary differential equation

$$\ddot{u}+p\dot{u}+qu=0, \qquad (3)$$

and we recognize the angular momentum $L=z\times\dot{z}=x\dot{y}-\dot{x}y\stackrel{def}{=}W[x,y]$ as these solutions' Wronskian! Newton's law (2) thus becomes

$$\frac{d}{dt}W=-pW, \qquad (4)$$

which is Abel's formula for the Wronskian. This concludes the justification of the claims made in the article's title, where "$=$" stands for "a special case of." Complexification—i.e., going from (3) to (1)—revealed something not seen in one space dimension.

MATHEMATICAL CURIOSITIES

*By Mark Levi*

### A Logical Question

An entirely different way to understand (4) is to observe that the divergence of any linear vector field is the logarithmic derivative of the area of a region carried by the field (there is no need to consider infinitesimal areas for linear flows). But the divergence of the vector field in the phase plane of (3) is $-p$, and thus the area $W$ of the parallelogram generated by two solution vectors satisfies $\dot{W}/W=-p$, as in (4).

The two aforementioned arguments, which are entirely different, lead to the same conclusion (4). Are these arguments homotopic? This is an interesting question for logicians.

### A Hidden Symmetry

Here is another puzzling connection between Abel's theorem and Noether's theorem on conserved quantities. Note that (1) is invariant under rotations; Noether's theorem applies in the conservative case ($p\equiv 0$) and guarantees conservation of the angular momentum $L=\text{const.}$, thus implying a special case of Liouville's theorem: $W=\text{const.}$ One could thus say that the cause is the symmetry hidden in (3) but revealed in (1).

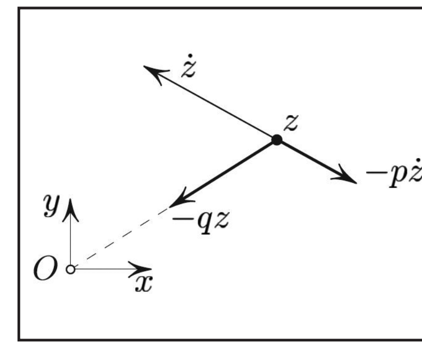


**Figure 1.** *Both coordinates of $z$ satisfy (3). Here, $p=p(t)$, $q=q(t)$. Figure courtesy of Mark Levi.*

*Mark Levi (levi@math.psu.edu) is a professor of mathematics at the Pennsylvania State University.*

# Model Uncertainty: Mathematical and Statistical

*By E. Bruce Pitman*

Mathematical models developed for computational simulation of complex, real-world processes are crucial ingredients in virtually every field of science, engineering, medicine, and business. The remarkable growth in computing power and the matching gains in algorithmic speed and accuracy have increased the applicability and reliability of simulations, making them faster and enabling their employment in previously intractable problems. Statistical models play a crucial role in analyzing real-world processes in virtually every field. The recent explosion in the storage and availability of data—and the computing power required to handle it—has increased the centrality of statistical analysis. A convenient way of categorizing models is to say that statistical models are useful for processes with abundant available data, and math models are valuable in data-poor environments.

It is rarely—perhaps never—possible to construct a mathematical or statistical model of a process with assurance (from its construction) that the model accurately represents all of the process's details. The crucial final step when utilizing a model for prediction or comprehension of a real-world process is to understand the uncertainties inherent in that model's use. Mathematicians and engineers call this process uncertainty quantification, which has become a major part of applied mathematics. Statisticians refer to it as model uncertainty (MU) — one of the most prominent fields of statistics.

In 2018-2019, the Statistical and Applied Mathematical Sciences Institute (SAMSI) hosted a year-long program called "Model Uncertainty: Mathematical and Statistical" (MUMS), with several workshops occurring throughout the year. SAMSI's central research activity involves working groups: collections of faculty visitors, postdoctoral fellows, and students with a shared interest in a particular topic or problem. The MUMS program generated both working groups with a more theoretical leaning and working groups of a more applied nature, and sponsored activities that fostered exchanges between the theoretical and applied. Programming activities in statistics, modeling, and computational mathematics illustrate MUMS' success and highlight some important problems in MU.

Mathematical modelers commonly formulate a large computer simulation of a physical or biological process, composed of a discretization of a system of ordinary differential equations (ODEs) and/or partial differential equations (PDEs). Meaningful data with which to judge a model requires fusion of results from computer simulations and experimental measurements. This approach gives rise to several questions. To begin, can one calibrate the model and determine good values for the important parameters in the system that are consistent with the data? Answering this question is predicated on determining which parameters are important — itself a difficult task. Next comes calibration, a procedure that typically involves a Markov chain Monte Carlo (MCMC) method to calculate the probability distribution for these parameters. MCMC demands many evaluations of the governing differential equations, meaning that constructing a surrogate for the governing system is often helpful.

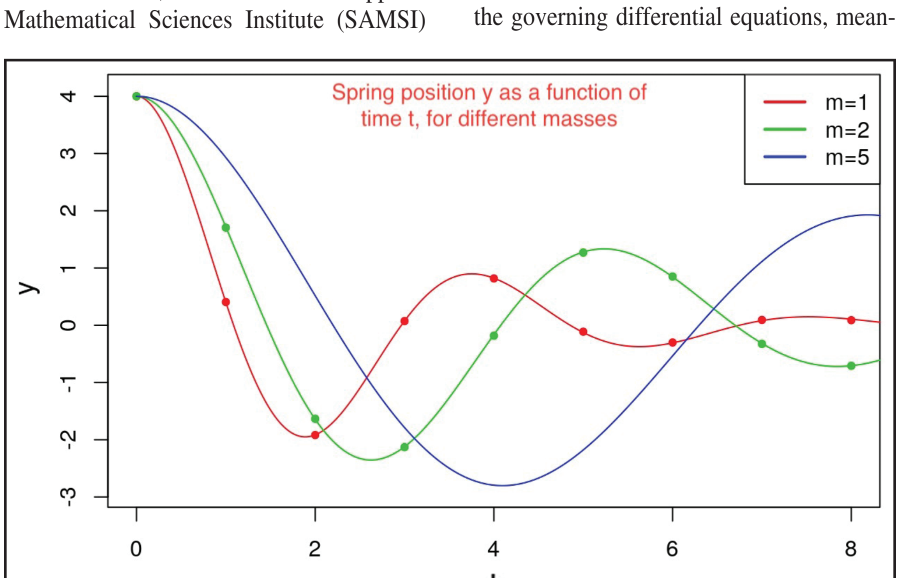


**Figure 1.** *Data for the damped spring experiment. Red and green dots show the position of the mass at times $t=1,\ldots 8$ for mass 1 and mass 2 respectively. The blue curve, which is not known to the analyst, indicates the position for mass = 5; the challenge is to predict the velocity at a specified time. Figure courtesy of E. Bruce Pitman and Pierre Barbillon.*

In statistics, Gaussian Stochastic Process (GaSP) emulators comprise the workhorse surrogate model. GaSP emulators are a nonparametric regression of data that are equipped with an estimate of the likely error of that regression. But when it comes to model behavior at a large number of space/time points, the typical GaSP construction is computationally intractable, thus necessitating new approaches. Efficient construction of a GaSP emulator for high-dimensional inputs and outputs—and the associated problem of finding reduced-order models for the system of interest—touched many of the working groups and represented a recurring theme throughout the year.

The preceding discussion makes a fundamental assumption: that the computed system of equations adequately represents the physical or biological processes being studied. A moment's reflection tells us that no mathematical model can capture every relevant process across all length and time scales. Thus, a somewhat more precise question is: Given a specified quantity of interest, does the mathematical model being computed satisfactorily represent the operative processes? That is, is the model system adequate for purpose?

Bob Moser (University of Texas at Austin) presented new ideas on this problem of model discrepancy to one of the working groups, which stimulated months-long discussions. Perhaps a simple example can illustrate the important questions at the heart of the challenge: the motion of a damped linear spring (see Figure 1). Moser asked participants to imagine a damped spring with a mass at its end, the wrinkle being that the constitutive relation for the damping is unknown. After receiving data consisting of the position of the mass at several times for mass values 1 and 2, one is asked to predict the velocity of the spring mass at a specified time for mass value 5. This problem presents two subtle issues. First, the data gives the position value at several times, but researchers are required to predict a latent variable: the velocity. Second, data is provided for values of the mass equal to 1 and 2, but the question seeks to extrapolate to mass 5.

Let us examine this problem a bit more deeply. Given the data, we model the mass's location at the $i^{\text{th}}$ time as

$$z_i=\zeta(t_i)+\epsilon_i,$$

where $\zeta$ is the true value of the spring extension for the correct input parameters and $\epsilon$ represents observation errors, assumed to be independent and normally distributed. A computational model of the spring system encodes conservation of mass and momentum with initial and boundary conditions. However, the constitutive relation between stress and stress rate—and strain and strain rate—is at best an approximation based on prior experiments. We believe that the conservation principles hold universally but know the constitutive law holds only in a limited range of conditions. It is here that model discrepancy comes into play [2-4]. We postulate an error due to model inadequacy (owing to the unknown damping relation):

$$\zeta(t)=\eta(t,\theta)+\delta(t). \qquad (1)$$

Here, $\theta$ is a set of calibration parameters that are not exactly known. Thus, our observation model is

$$z_i=\eta(t_i,\theta)+\delta(t_i)+\epsilon_i. \qquad (2)$$

That is, the observation is a sum of the "true" value of the system, an error due to model inadequacy, and measurement error. The classic Kennedy and O'Hagan framework [4] models $\delta$ as a GaSP, assigns a prior to $\theta$, and determines posterior distributions conditioned on the observed data.

Moser described ideas published in [5], wherein a discrepancy operator is postulated and embedded in the dynamical system. An earlier example of this idea contains the damped spring-mass scenario [6]. Because the actual damping is unknown, including model inadequacy attempts to rectify this constitutive ignorance. The embedded discrepancy operator contains several parameters that must also be calibrated, adding to the burden of analysis.

An alternative approach to representing model error provides moment-based likelihoods through a generalized polynomial chaos expansion [7]. Assuming that the form of model discrepancy continues to hold, the chaos expansion can be valuable when attempting to make predictions for parameters outside of range testing.

A different approach to studying dynamic discrepancy considers the suspect parameters as varying in time and adds a dynamic discrepancy: $\delta(x,\chi(t))$. One may assume a Gaussian process prior, which turns the governing ODEs or PDEs into a system of stochastic differential equations [1]. Dave Mebane (West Virginia University) presented this idea at the 2019 Materials and

*See* **Model Uncertainty** *on page 8*

# Preconditioning in the New Decade

*By Edmond Chow and Kees Vuik*

The subject of preconditioning, which encompasses techniques that help accelerate the convergence of iterative linear solvers, is already decades old. Yet the design and study of preconditioners seems constantly fresh as it continues to address problems from new application domains, adapts to new computer architectures, and incorporates ideas from new fields.

Preconditioning research is inherently interdisciplinary; therefore, the design of preconditioners must often be closely tied to the applications from which the equations arise, which poses a challenge for the field. No black box preconditioners work well for all problems, and preconditioning researchers must substantially understand domain applications to exploit the structure and properties of the matrices that emerge from them.

Some of the newest applications that demand preconditioners to address large-scale instances do not originate directly from partial differential equations (PDEs). For example, problems based on integral equation formulations, Gaussian process regression, and biomolecular simulations give rise to matrices whose entries represent the interactions between sets of points. When the interactions—defined by so-called kernel functions—are long-ranged, the matrices are dense but possess intriguing hierarchical low-rank structure, sometimes called data sparsity (see Figure 1). Fast linear-time matrix-vector multiplication algorithms are applicable for matrices with such structure, thus making iterative solution methods a viable choice. Some solution methods exist for certain types of rank-structured matrices—which could act as preconditioners—but otherwise the issue of preconditioning for these problems is new ground for exploration.

Although preconditioning traditionally applied only to linear systems of equations, it is now proving useful in the context of nonlinear equations. Few current ideas pertain to a nonlinear equation's transformation into an equivalent one that is more rapidly solvable by a Newton method. Mathematician Martin Gander suggests viewing nonlinear preconditioning as a fixed-point iteration but employing Newton's method to solve the equations at the fixed point (rather than using the fixed-point iteration as a solver). This is akin to taking the Jacobi or Gauss-Seidel fixed-point iterations and utilizing their splittings as preconditioners for Krylov subspace methods in the linear case.

Like other algorithms that must run efficiently on parallel computers, preconditioning has constantly adapted to new computer architectures. Graphics processing units (GPUs) and other hardware accelerators have high compute and memory bandwidth capabilities, but the question on how to efficiently use this hardware for the sparse computations typically required in preconditioning remains open. New preconditioning algorithms may very well need to exploit low-precision computational units available on the newest GPUs; because preconditioners are approximate anyway, computing and applying them in low precision is a possibility.

Designing preconditioners for realistic problems is sometimes as much an art as it is a science. Scientists have used machine learning to choose from the many options for preconditioners and select any necessary parameters. One could also possibly use machine learning to construct preconditioners him/herself. Early applications of neural networks included solving the linear systems from discretized PDEs, but these were quite primitive. It remains to be seen how machine learning can provide techniques where preconditioning theory is lacking for many realistic and complex problems.

These are just some of the issues that researchers are considering in the new decade. As preconditioning techniques are established for specific problems, domain scientists are demanding preconditioning for larger problems, more complicated physics, and novel problems altogether. This continuous cycle has kept preconditioning research active and alive. Preconditioning presents numerous opportunities to help accelerate the myriad of computational tools that advance science and engineering.

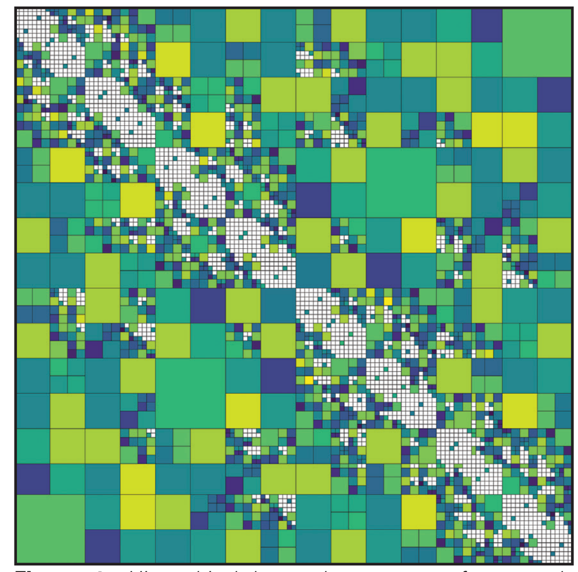

**Figure 1.** *Hierarchical low-rank structure of a sample matrix. Brighter colors correspond to higher rank. Figure courtesy of Lucas Erlandson.*

The International Conference on Preconditioning Techniques for Scientific and Industrial Applications, to be held in summer 2021 at the Chemnitz University of Technology in Germany, should be of interest to those in the field.

*Edmond Chow is an associate professor in the School of Computational Science and Engineering at the Georgia Institute of Technology. He previously held positions at D. E. Shaw Research and Lawrence Livermore National Laboratory. Kees Vuik is a professor of numerical analysis at the Delft University of Technology. His expertise is the development of new preconditioners and high-performance computing.*



# SIAM Weighs in on Federal Research Priorities

*By Ben Kallen*

SIAM's Washington liaisons have been actively engaging with both President Trump's administration and Congress on emerging federal priorities—including new fields of research—through responses to various requests for information (RFIs). Such efforts alert federal audiences to the vital role of applied mathematicians and computational scientists in driving advances in critical and societally relevant areas of science and technology. Individual efforts focused on White House initiatives for strategic computing and the bioeconomy, as well as the House Select Committee on the Climate Crisis.

### National Strategic Computing Initiative

SIAM offered recommendations to the White House to inform the administration's attempts to update the National Strategic Computing Initiative (NSCI), which guides federal investments in supercomputing. SIAM provided this input in response to an RFI from the White House in July 2019 to inform changes to NSCI objectives. SIAM recommended strengthening the NSCI by addressing specific research and workforce gaps. Central to SIAM's RFI feedback was the premise that the health and vitality of the entire strategic computing ecosystem depends not only on the speed and availability of supercomputing systems, but also on the foundational research advancements generated by the applied mathematics and computational science communities. SIAM's comments also contended that an updated NSCI must support a workforce development pipeline that expands opportunities for students and early career researchers; this would strive to meet the national need for scientists and software developers capable of devising modeling and simulation methods tailored to exploit forthcoming computing systems.

### Bioeconomy

The White House issued an additional RFI requesting input on ways in which the federal government can support the burgeoning bioeconomy. The administration described the bioeconomy as "the infrastructure, innovation, products, technology, and data derived from biologically-related processes and science that drive economic growth, promote health, and increase public benefit." In its response, SIAM provided detailed descriptions of the role that mathematics, modeling, and computational sciences can play in this area. The reply specifically discussed the importance of predictive science and the integration of data into all aspects of biological research, including biomedical and agriculture applications. SIAM's comments also included structural suggestions such as comprehensive data initiatives (especially in biomedical research), transparent science and results enabled by supporting the value of scientific publications and intellectual property, and data sharing across agencies to accelerate scientific breakthroughs.

### Mitigating Against Climate Change

In October, the House Select Committee on the Climate Crisis released an RFI soliciting ideas for future recommendation policies that Congress can pursue to address the climate crisis. SIAM highlighted the role of modeling in predicting the effects of climate change and effectively mitigating damaging outcomes. For example, the Dutch government used modeling and simulation to dictate precise modifications to the country's seaside dikes in order to prevent flooding. This targeted approach improved infrastructure resilience to climate change and saved billions of euros. SIAM also considered cross-cutting issues like power grid optimization, computational design of sustainable and long-lasting materials, and potential models of climate change's impact on human health. The American Mathematical Society signed onto this response, thus helping to expand its support base.

SIAM's feedback to these RFIs open potential new avenues for engagement with policymakers and novel opportunities for the society to ensure that its priorities are included in broader discussions of science and engineering policy. For instance, the SIAM Committee on Science Policy met this past fall—following the submission of SIAM's reply to the bioeconomy RFI—with the official leading bioeconomy efforts at the White House.

*Ben Kallen is a government relations associate at Lewis-Burke Associates LLC.*

# Benjamin Franklin, Andrew Carnegie, and Other Friends of SIAM

*By Ken Boyden*

Charitable giving in the U.S. has a long and distinguished history, dating as far back as the 1636 founding of Harvard College with support from the Massachusetts Puritans, and the 1727 creation of "Junto," an exclusive social club established by Benjamin Franklin that discussed philanthropic ideas for "the love of mankind in general." In more modern times, we associate philanthropy with Andrew Carnegie and John D. Rockefeller, the Ford and MacArthur Foundations, and the Gates-Buffett Pledge, which encourages many of the world's ultra wealthy to commit 50 percent of their estate assets to charity. Indeed, numerous leading 501c3 charitable organizations currently rely on philanthropic generosity to grow and prosper.

Fundraising to support SIAM, our mission, and our work involves a far more proactive strategy than awaiting the passing of our friends and supporters before learning about bequests or testamentary trusts to the society in their estate plans. While we are always extraordinarily grateful to be included in estate plans through any deferred giving vehicle, we much prefer to learn of such important and impactful expressions of support during the lives of our donors.

It is with the philanthropic support of our global donors that SIAM strives to enable and advance its core purpose to build cooperation between mathematics and the worlds of science and technology. Through the recent addition of the position of Director of Development and Corporate Relations, SIAM leadership has made a tangible commitment to solicit and professionally manage donations, celebrate and recognize our donors' generosity, and grow support for our priority areas. These priorities include the growth of endowment funds to ensure in perpetuity the continuation of our Visiting Lecturer Program and various prizes; ongoing student travel funding; professional development and fellowship programs; production of leading publications; and continuing policy work and advocacy.

Gifts of all types impact this effort. In addition to estate plans, outright donations in more traditional forms such as cash, checks, or credit cards are the most common type of annual gift that SIAM receives. Larger gifts typically involve a meeting and conversation with the donor to ensure our understanding of the donation's purpose and ascertain that its use will stay true to both the donor's wishes and SIAM's mission.

Of course, we are happy to discuss in confidence the wishes of any donor who is considering a planned bestowal such as a bequest, trust, charitable gift annuity, real estate contribution, retirement account beneficiary distribution, appreciated security, insurance, or even the gifted rights to intellectual property. Friends of SIAM who have previously made estate provisions that included SIAM without advance notification before their passing have been truly influential; we only regret the missed opportunity to say "thank you" during their lifetime.

SIAM's mission and work have surely played a significant role in virtually all innovations related to healthcare, communications, aerospace, data science, and climate research, among other areas. The continued support of our members and allies assures SIAM's enduring leadership role as the fields of applied and industrial mathematics doggedly pursue resolutions to the persistent problems of society at large. Moreover, SIAM's positive impact on the scientific lives and careers of its members has helped further applied mathematics and other related disciplines.

Please consider supporting SIAM with your generosity today and in the future. Your financial assistance will help us advance the application of mathematics and computational science to engineering, industry, science, and society. Similarly, your support will allow us to continue to foster the exchange of ideas and promote research that yields effective mathematical and computational methods and techniques.

If you wish, let us know of your plans. We are always happy to meet with our friends. Read more about donating[1] or email me directly at boyden@siam.org.

*Ken Boyden, Esquire is the Director of Development and Corporate Relations at SIAM.*

[1] https://www.siam.org/donate

# SIAM Membership Celebrates Many Milestones

*By Tim Fest*

2019 was a banner year for SIAM Membership, which welcomed more than 1,450 nonstudent members to SIAM's global community of applied mathematicians and computational scientists. This growth raised our nonstudent membership total to a new high of 8,545 members, and set first-time records for early career members (450 new members for a total of 1,330) and members from countries that qualify for Outreach Membership[1] (401 new members for a total of 952).

New members strengthen and expand the SIAM community by bringing novel perspectives, experiences, and insights. Their effect on the society is cumulative, and the impact of additional members is far greater than just the sum of its parts.

SIAM has been growing in other ways as well. The addition of the new SIAM Activity Group on Applied and Computational Discrete Algorithms (SIAG/ACDA) brings the total count of activity groups to 22. Furthermore, SIAM has embraced data science with the new *SIAM Journal on Mathematics of Data Science* (*SIMODS*)[2] and the SIAM Conference on Mathematics of Data Science (MDS20).[3] The first iteration of the latter is co-located with the SIAM International Conference on Data Mining (SDM20) in Cincinnati, Ohio this May. Both *SIMODS* and MDS20 are worthwhile expansions into this cutting-edge field that has seen unprecedented progress over the last decade.

SIAM has also expanded and improved its relationships with peer societies through reciprocal agreements. Members of the János Bolyai Mathematical Society in Hungary and the Unione Matematica Italiana in Italy can now join SIAM at a 30 percent discount. We have also added a new North American reciprocal society: the National Association of Mathematicians (NAM). NAM is a professional association for mathematicians in the U.S., especially African Americans and other minorities.

We continue to seek ways to break down barriers so our members can engage across borders, disciplines, and career levels, and we're looking forward to announcing several big projects in 2020 to keep the momentum going. But the most important factor in SIAM's membership growth is the members who are reading this article today. Without your continued patronage by renewing your membership; volunteering on committees; running for elected office; serving as editors for—and reading and submitting to—SIAM journals; supporting SIAM conferences by organizing, attending, or submitting content; and recommending SIAM to friends, colleagues, and students, SIAM would not be the healthy, robust organization that it is today.

*Tim Fest is SIAM's Membership Manager and a Certified Association Executive.*

[1] https://www.siam.org/membership/join-siam/individual-members/outreach-membership
[2] https://www.siam.org/publications/journals/siam-journal-on-mathematics-of-data-science-simods
[3] https://www.siam.org/conferences/cm/conference/mds20

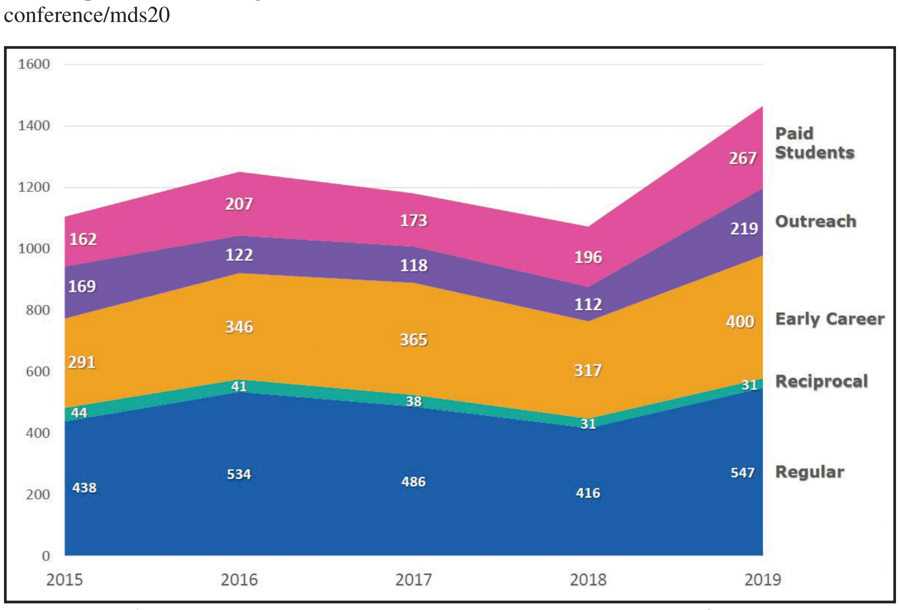


*Breakdown of the more than 1,450 new nonstudent members that joined SIAM in 2019, which brought nonstudent membership to a record high of 8,545. Figure courtesy of Tim Fest.*

## Model Uncertainty

*Continued from page 6*

Data Science Hackathon,[1] sponsored by SAMSI and the Data-enabled Science and Engineering of Atomic Structure group at North Carolina State University.

Imagine a system of two equations that take the form

$$\frac{\partial x}{\partial t} = v;$$

$$\frac{\partial v}{\partial t} = -c(\chi)v - kx + \delta(x, \chi(t), \beta),$$

where $\beta$ are hyperparameters of the Gaussian process. If more than one parameter is suspect, expanding them all can explode the number of terms to be determined. Therefore, a low-order Karhunen-Loève or polynomial chaos expansion is often specified to reduce the work.

Pierre Barbillon (AgroParisTech) illustrated yet another approach at the MUMS Transition Workshop.[2] In our joint work, he extends the governing system by postulating a stochastic relaxation. The governing equations take the form of a generalized mean-reverting process with a random forcing. The spring-mass system becomes

$$\frac{\partial x}{\partial t} = v; \qquad m\frac{\partial v}{\partial t} = w$$

and

$$\frac{\partial w}{\partial t} = -\frac{1}{\tau}(w - (-cv - kx)) + \sigma^2\frac{\partial B}{\partial t}.$$

Here we abuse notation in writing $\partial B/\partial t$, where $B$ is Brownian motion. Notice that in the zero-relaxation limit $\tau \to 0$, the auxiliary variable $w \to -(cv+kx)$ formally, thus recovering the original ODEs. Simulations allow this system to wander away from the (inadequate) constant coefficient linear spring; calibration of $\tau$ and $\sigma^2$ suggest the magnitude of this discrepancy.

This example of model inadequacy suggests important issues of model and variable selection (the focus of another working group). It highlights the need for a close collaboration between domain scientists, statisticians, and computational and applied mathematicians to evaluate MU in a way that allows quantification of the uncertainty in predictions, which is the investigation's ultimate goal.

[1] https://www.samsi.info/programs-and-activities/year-long-research-programs/model-uncertainty-mathematical-statistical-mums/samsi-co-sponsored-event-mums-materials-and-data-science-hackathon/
[2] https://www.samsi.info/programs-and-activities/year-long-research-programs/model-uncertainty-mathematical-statistical-mums/mums-transition-workshop-and-spuq-may-14-17-2019/

### References

[1] Bhat, K.S., Mebane, D.S., Storlie, C.B., & Mahapatra, P. (2017). Upscaling uncertainty with dynamic discrepancy for a multi-scale carbon capture system. *J. Amer. Stat. Assoc.*, *112*, 1453-1467.

[2] Brynjarsdottir, J., & O'Hagan, A. (2014). Learning about physical parameters: The importance of model discrepancy. *Inv. Prob.*, *30*(11).

[3] O'Hagan, A. (2013). Bayesian inference with mis-specied models: Inference about what? *J. Stat. Plan. Infer.*, *143*, 1643-1648.

[4] Kennedy, M.C., & O'Hagan, A. (2001). Bayesian calibration of computer models. *J. Roy. Soc. Stats. B*, *63*, 425-464.

[5] Morrison, R., Oliver, T., & Moser, R.D. (2016). Representing model inadequacy: A stochastic operator approach. *SIAM J. Uncert. Quant.*, *6*, 457-496.

[6] Oliver, T., Terejanu, G., Simmons, C.S., & Moser, R.D. (2015). Validating predictions of unobserved quantities. *Comp. Meth. Appl. Mech. Eng.*, *283*, 1310-1335.

[7] Sargsyan, K., Huan, X., & Njam, H.N. (2018). Embedded model error representation for Bayesian model calibration. *Int. J. Uncert. Quant*.

*E. Bruce Pitman is a professor in the Department of Materials Design and Innovation at the University at Buffalo. He chaired the organizing committee for the 2018-2019 "Model Uncertainty: Mathematical and Statistical" program at the Statistical and Applied Mathematical Sciences Institute.*